

# Deposition of NCD films using hot filament CVD and Ar/CH<sub>4</sub>/H<sub>2</sub> gas mixtures

P.W. May <sup>a,\*</sup>, J.A. Smith <sup>a</sup>, Yu. A. Mankelevich <sup>b</sup>

<sup>a</sup> School of Chemistry, University of Bristol, Bristol BS8 1TS, U.K.

<sup>b</sup> Nuclear Physics Institute, Moscow State University, 119992 Moscow, Russia

Available online 31 August 2005

## Abstract

Ar/CH<sub>4</sub>/H<sub>2</sub> gas mixtures have been used in an attempt to deposit nanocrystalline (NCD) diamond and ultra-nanocrystalline (UNCD) diamond films using hot filament (HF) chemical vapour deposition (CVD). A detailed composition map has been developed for the type of films deposited in the Ar/CH<sub>4</sub>/H<sub>2</sub> system. It was found that the standard gas mixtures of 1%CH<sub>4</sub>/Ar (+1–2%H<sub>2</sub>) that are used successfully to grow UNCD films in microwave plasmas produce only graphitic film growth in a HF system. A 2-dimensional computer model was used to calculate the gas phase composition for these conditions. The non-uniform temperature distribution arising from the hot filament produces a substantial decrease in gas phase H atoms near to the substrate surface, whilst [CH<sub>3</sub>] remains almost constant. We find that the [H]:[CH<sub>3</sub>] ratio near the surface decreases from ~5:1 for 1%CH<sub>4</sub>/H<sub>2</sub> gas mixtures to 1:36 for 1%CH<sub>4</sub>/Ar mixtures, and that this can explain the decrease in growth rate and the reduction in film quality toward nanocrystalline or graphitic films. Increasing the H<sub>2</sub> content in the gas mixture improves the situation, but NCD growth was confined to a limited composition window at the boundary of the microcrystalline diamond growth region and ‘no growth’ region. A 2D model of a microwave CVD system has also been developed which gives the gas phase composition for the various Ar-rich gas mixtures. We find that due to the higher temperatures within the plasma ball, plus the fact that the gas temperature close to the substrate surface is in excess of 2000 K ensures that the [H]:[CH<sub>3</sub>] ratio remains  $\gg 1$ , and thus permits growth of diamond, NCD or UNCD. Furthermore, since the model shows that [CH<sub>3</sub>] and [C<sub>2</sub>H] are always much greater than [C<sub>2</sub>], this suggests that CH<sub>3</sub> and C<sub>2</sub>H species may be more important growth precursors than C<sub>2</sub> under typical UNCD deposition conditions.

© 2005 Elsevier B.V. All rights reserved.

**Keywords:** Nanocrystalline diamond; Hot filament CVD; Ar/CH<sub>4</sub>/H<sub>2</sub> gas mixtures

## 1. Introduction

Diamond films can be deposited using a chemical vapour deposition (CVD) process involving the gas phase decomposition of a gas mixture containing a small quantity of a hydrocarbon in excess hydrogen [1]. A typical gas mixture uses 1%CH<sub>4</sub> in H<sub>2</sub>, and this produces polycrystalline films with grain sizes in the micron or tens of micron range, depending upon growth conditions, substrate properties and growth time. The gas mixture can be activated in a number of ways, such as microwave (MW) plasma, combustion

torch, or a hot metal filament. The appearance and properties of the microcrystalline diamond (MCD) films produced by each method are very similar, since with all these methods the gas phase chemistry is very similar. This is because the initial reactant gases are converted to approximately the same steady-state mixture of hydrocarbon fragments and hydrogen atoms above the growing surface [2,3]. The Bachmann diagram [4] indicates that, due to this similarity in steady-state chemistry, MCD deposition only depends upon the ratios of C:H:O in the input gases, and not on their specific chemical identities.

A high concentration of hydrogen atoms close to the substrate surface is crucial in the deposition process, since H performs a number of important functions. First, H atoms can etch surface graphitic (sp<sup>2</sup>) carbon many times faster

\* Corresponding author. Tel.: +44 117 9289927; fax: +44 117 9251295.

E-mail address: paul.may@bris.ac.uk (P.W. May).

than diamondlike ( $sp^3$ -bonded) carbon. Second, the H atoms help to terminate the ‘dangling bonds’ on the diamond surface, thus stabilising the surface while growth takes place. Also, the H atoms react with large gas phase hydrocarbon fragments, splitting them into small pieces thus preventing polymer build-up. Finally, atomic H creates radical sites on the surface by undergoing H-abstraction reactions, removing some of the terminal hydrogens. It is generally believed [5,6] that the main growth species in standard CVD diamond growth is the  $CH_3$  radical, which adds to the diamond surface stepwise following successive hydrogen abstraction by H atoms. Thus, a high concentration of atomic H at the surface is a prerequisite for successful MCD deposition.

By increasing the ratio of methane in the standard  $CH_4/H_2$  gas mixture from 1% to  $\sim 5\%$ , the grain size of the films decreases, and eventually becomes of the order of hundreds down to tens of nanometres. Such nanocrystalline diamond (NCD) films (often termed ‘cauliflower’ or ‘ballas’ diamond) are smoother than the microcrystalline ones, but have larger numbers of grain boundaries that contain substantial graphitic impurities. With further addition of  $CH_4$ , the films become graphitic.

Recently, so-called ultra-nanocrystalline diamond (UNCD) films have become a topic of great interest, since they offer the possibility of making smooth, hard coatings at relatively low deposition temperatures, which can be patterned to nanometre resolution [7]. These differ from NCD films, since they have much smaller grain sizes ( $\sim 2\text{--}5$  nm), and have little or no graphitic impurities at the grain boundaries. Most reports of the deposition of these films describe using a microwave plasma CVD reactor and gas mixture of 1% $CH_4$  in Ar, usually with addition of 1–5%  $H_2$ . Addition of nitrogen to the plasma during CVD has been found to give the films characteristics that are similar to n-type semiconductors, suggesting possible applications in electronic devices. However, the fundamental growth mechanism of these UNCD films is still unclear. Originally it was suggested [8] that the  $C_2$  radical played an important role in the growth mechanism. However, recent work by ourselves [9] and others [10] have cast doubt on the veracity of this  $C_2$  mechanism. It now seems more likely that it is a delicate balance between the concentrations of  $CH_3$  and  $C_2$  (and/or  $C_2H$ ) radicals close to the substrate surface that determines the growth morphology and hence the properties of the resulting film.

To date, there has only been one report of the use of similar  $Ar/CH_4/H_2$  gas mixtures to deposit NCD (or UNCD) in a hot filament (HF) reactor [11]. In that report, the compositional diagram for mixtures of Ar,  $CH_4$  and  $H_2$  was mapped out corresponding to the type of film grown. It was found that for  $CH_4/H_2$  concentrations below 1% (in the presence of Ar) no growth was observed, whereas MCD was deposited for  $CH_4/H_2$  concentrations between 1% and 5% and  $Ar/H_2$  concentrations between 0% and 95%. Higher concentrations of methane generally led to non-diamond

growth. NCD deposition occurred only in a very narrow gas composition window,  $CH_4/H_2=2\text{--}5\%$  and  $Ar/H_2=95.5\text{--}98\%$ , and this gave diamond films with grain size  $\sim 50$  nm and high phase purity. However, these gas mixtures are still relatively hydrogen-rich compared to the 1% $CH_4/Ar$  (+1–2% $H_2$ ) mixtures that are used to deposit UNCD films in MW reactors.

In this paper we report attempts to deposit NCD and UNCD films in a hot filament reactor using  $Ar/CH_4/H_2$  gas mixtures, both in hydrogen-rich and hydrogen-poor environments. We also use 2-dimensional modelling of the gas chemistry in both hot filament and microwave reactors to attempt to understand the observations, and finally to show how the experimental and theoretical data may help to shed some light on the (U)NCD growth mechanism.

## 2. Experimental

Films were deposited using a standard hot filament reactor operating at a pressure of 100 Torr using high purity Ar,  $CH_4$  and  $H_2$  as source gases. Mass flow controllers were used to vary the ratios of the 3 gases:  $[CH_4]/([CH_4]+[H_2])$  between 1% and 100% and  $[Ar]/([Ar]+[H_2])$  between 0% and 100%, with the flow of  $CH_4$  being constant at 1 sccm throughout (i.e. the flows of the other gases, and the total gas flow were changed accordingly). This was in order to keep the number of carbon atoms entering the chamber constant, so as to compare growth rates and film properties reliably. The filament was made from a 0.25 mm-diameter Ta wire, wound around a 3 mm-diameter core to produce a 2 cm-long coil that was positioned 5 mm from the substrate surface. Due to the higher thermal conductivity of  $H_2$  compared to Ar, for  $H_2$ -rich gas mixtures a higher filament current ( $\sim 6.5$  A) was required, as compared to Ar-rich gas mixtures (4–5 A), to achieve the same filament temperature of 2400 °C (monitored using a 2-colour optical pyrometer). The substrate was single crystal Si (100) which had been manually abraded prior to deposition using 1–3  $\mu m$  diamond grit, and then ultrasonically cleaned with propan-2-ol. The substrate sat on a separate heater to give additional uniform heating and to maintain it at a temperature of  $\sim 850\text{--}900$  °C (also measured using the optical pyrometer). Typical deposition times were 8 h, although some runs at higher methane concentrations were abandoned early due to premature filament breakage. For methane concentrations above 5% it was found that the filament would become covered with a thick, smooth, rounded coating after a period of 1 or 2 h (see Fig. 1(a)). This coating reduced the efficiency of the filament, and along with an increase in resistance, this meant that a higher current was needed to maintain the same temperature. Eventually the current required became so large that the filament failed. Laser Raman analysis of this coating gave a

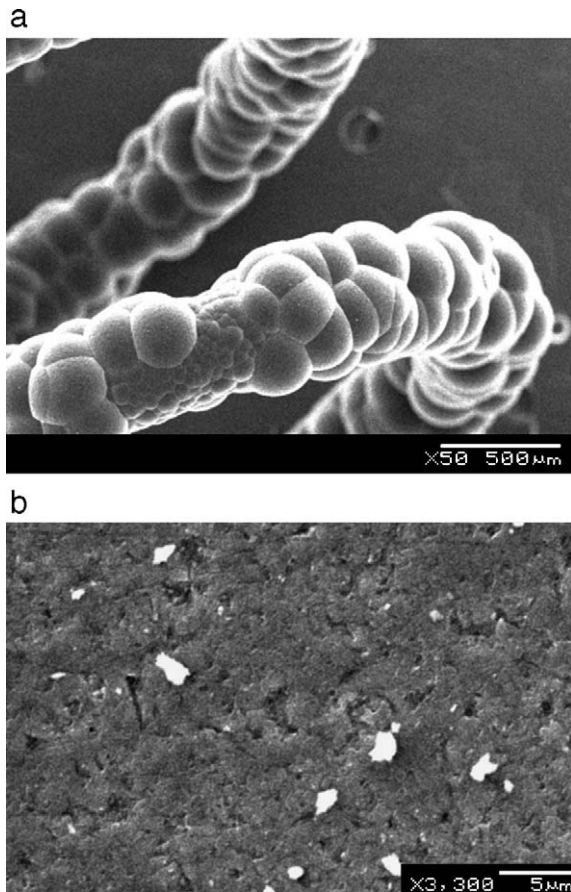


Fig. 1. (a) A SEM micrograph of the graphitic coating seen on the Ta filament after a 3 h growth in a 1%CH<sub>4</sub>/Ar gas mixture. (b). A SEM micrograph of the isolated nanoparticles seen on the Si surface after an 8 h growth in a 20%CH<sub>4</sub>/(CH<sub>4</sub>+H<sub>2</sub>), 99.4%Ar/(Ar+H<sub>2</sub>) gas mixture.

spectrum characteristic of crystalline graphite. After deposition the films were analysed by UV (325 nm) laser Raman spectroscopy and scanning electron microscopy (SEM).

### 3. Modelling

In order to understand the gas phase chemistry occurring in the CVD chamber, the composition of the gas mixture was calculated using an existing 2D and 3D model that has been specifically tailored to a reactor of this geometry [12]. The models comprise three blocks, which describe (i) activation of the reactive mixture (i.e. gas heating and catalytic H atom production at the filament surface), (ii) gas phase processes (heat and mass transfer and chemical kinetics), and (iii) gas-surface processes at the substrate. The gas phase chemistry and thermochemical input is taken from the GRI-Mech 3.0 detailed reaction mechanism for C/H/Ar gas mixtures [13]. As in previous studies [14–16] the conservation equations for mass, momentum, energy, and species concentrations, together with appropriate initial and boundary conditions, thermal, and caloric equations of state, are each integrated numerically until steady-state conditions are attained. This yields spatial distributions of the gas temperature,  $T_{\text{gas}}$ , the flow field, and the various species number densities and mole fractions.

We have also developed a model of plasma-chemical kinetics and heat and mass transfer to allow a full 2D simulation of the same gas mixtures in a MW reactor. Parameters for the model are taken from experimental observations of the shape and size of the plasma ball in our Astex-style microwave reactor operating at 800 W, with different Ar/CH<sub>4</sub>/H<sub>2</sub> gas mixtures. For example, an 800 W 1%CH<sub>4</sub>/2%H<sub>2</sub>/97%Ar plasma at 100 Torr produced a plasma ball that is roughly hemispherical (radius ~2.5 cm) and positioned ~1 mm above the substrate. A full description of the model and its comparison with experimental MW plasmas will be given in a later paper [17] but, briefly, the set of non-stationary conservation equations for mass, momentum, energy and species concentrations were solved numerically in cylindrical ( $r, z$ ) coordinates. Electro-

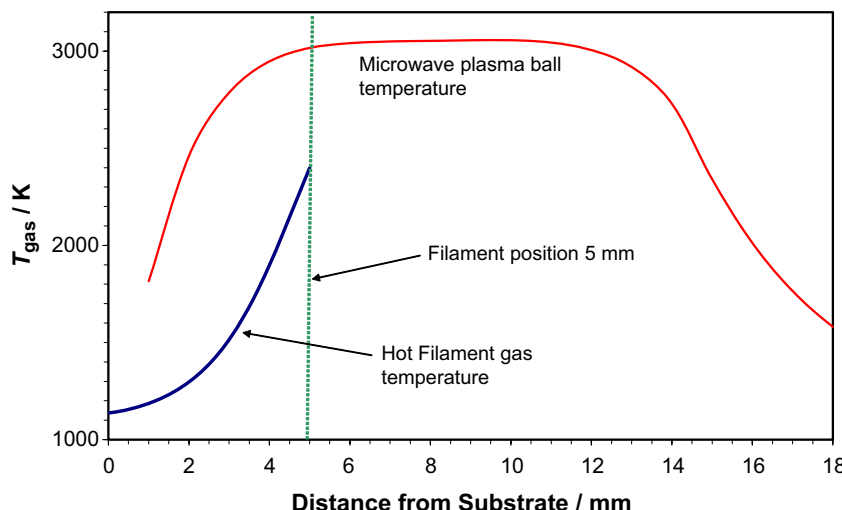


Fig. 2. Gas temperatures for the hot filament system ( $T_{\text{sub}}=1130$  K and substrate–filament distance=5 mm) and MW plasma system (800 W, 100 Torr), calculated by solving the 2D energy conservation equations in the model for the gas mixture in both our reactors, and for 1%CH<sub>4</sub>/2%H<sub>2</sub>/Ar gas mixture.

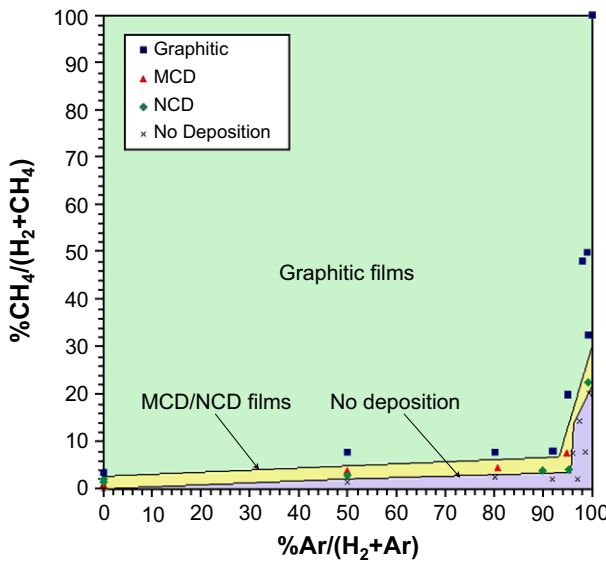


Fig. 3. An experimental composition map of the Ar/CH<sub>4</sub>/H<sub>2</sub> gas mixture for a hot filament reactor. The plotted points are from growth experiments, and the positions of the boundary lines between the 3 regions have been estimated from these. Key: ‘Graphitic’ means either that the films were predominantly sp<sup>2</sup> carbon in character (as determined by Raman spectroscopy) or that the filament became coated in a graphitic layer preventing film deposition. ‘MCD’ means microcrystalline diamond, giving a well resolved 1332 cm<sup>-1</sup> Raman line and faceted crystallite sizes >0.1 μm. ‘NCD’ means nanocrystalline diamond, and were films that appeared amorphous or had crystallite sizes <0.1 μm, but which also exhibited the 1150–1190 cm<sup>-1</sup> Raman line (see Fig. 5). ‘No Deposition’ is where no obvious films were deposited after 8 h of growth, although in some cases isolated crystallites were observed lying on top of the substrate.

magnetic fields are not calculated in this approach. Instead, a uniform electron temperature, T<sub>e</sub>, and absorbed power density are applied to a hemisphere approximately corresponding to the observed experimental plasma region. T<sub>e</sub>

values in the range of 1.3–1.5 eV for 1%CH<sub>4</sub>/H<sub>2</sub> and 2.4–2.7 eV for 1%CH<sub>4</sub>/2%H<sub>2</sub>/97%Ar were chosen using an electron and plasma kinetic 0D model to be consistent with experimental input powers of ~800 W. In the 0D model, the balance equations for charged and neutral species are solved for given reduced electric fields. Simultaneously, the electron energy distribution function for the chosen gas mixture composition is calculated by solving the Boltzmann equation with a two-term approximation and local field approach, using a set of known electron-particle collision cross-sections [18]. As a result, the steady-state species number density distributions, T<sub>e</sub>, and rate coefficients of electron reactions as a function of T<sub>e</sub> are obtained. Established plasma-chemical mechanisms (~35 species and ~300 reactions for H/C/Ar mixtures [19,20]) together with the electron temperature dependence of the electron collision processes are used in the 2D model of the microwave reactor.

Two tests show that this model gives what appears to be a realistic description of the plasma processes. First, the calculated number density for the C<sub>2</sub> radical in the centre of the plasma ball for a 1%CH<sub>4</sub>/2%H<sub>2</sub>/97%Ar gas mixture (100 Torr, 800 W) is ~10<sup>12</sup> cm<sup>-3</sup>, which agrees closely with experimental measurements from similar plasmas [10]. Second, the calculated gas temperature in the centre of the plasma is 3000 K, dropping to <1800 K close to the substrate (see Fig. 2). This is consistent with measurements of the gas temperature (usually taken from rotational temperatures of C<sub>2</sub>) in similar Ar/CH<sub>4</sub>/H<sub>2</sub> plasmas [9,10,21].

#### 4. Results

Fig. 3 shows a composition map for the Ar/CH<sub>4</sub>/H<sub>2</sub> system in our HF reactor. This broadly resembles the results

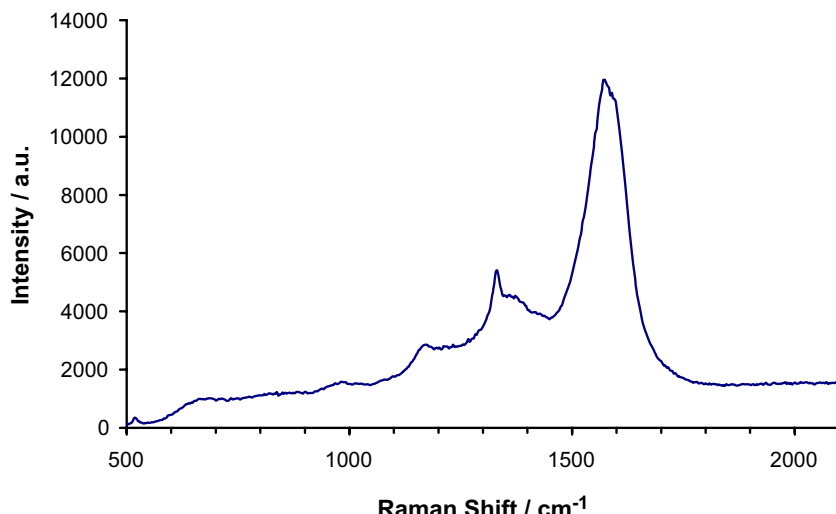


Fig. 4. Laser Raman (325 nm) spectrum from a film deposited with [CH<sub>4</sub>]/([CH<sub>4</sub>]+[H<sub>2</sub>])=4% and [Ar]/([Ar]+[H<sub>2</sub>])=90% at 100 Torr pressure, showing the presence of the 1150–90 cm<sup>-1</sup> peak associated with NCD, plus a discernible diamond peak at 1332 cm<sup>-1</sup> and broad G and D bands.

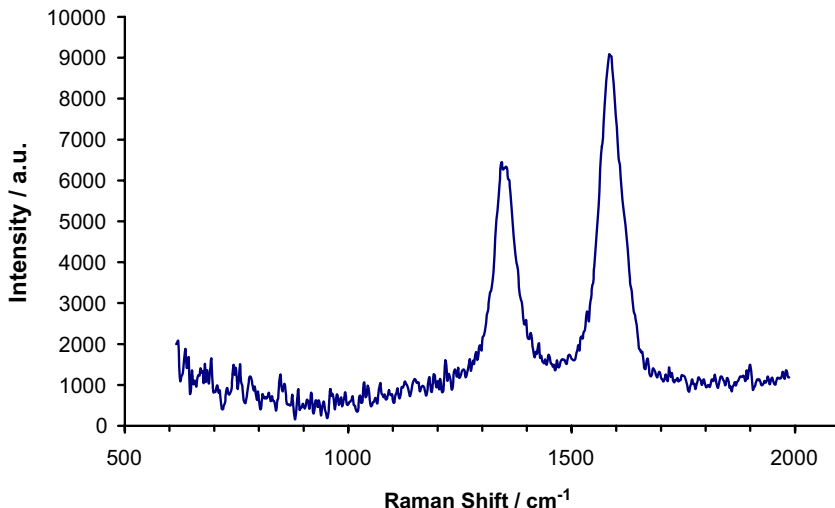


Fig. 5. Laser Raman (514 nm) spectrum from a film deposited with 1%CH<sub>4</sub>/Ar at 100 Torr pressure, characteristic of crystalline graphite.

of Lin et al. [11], in that there is only a narrow composition range in which MCD or NCD is deposited. Generally, if the methane concentration becomes too high the filament becomes coated in a graphitic layer inhibiting gas activation and thus stopping subsequent film growth. Any films that are deposited consist of graphitic or non-diamond carbon. With low concentrations of methane, no film growth is seen (or the growth rate is too low to discern growth in a deposition time of 8 h). Diamond films are deposited only in a very narrow region around  $[\text{CH}_4]/([\text{CH}_4] + [\text{H}_2]) \sim 1\text{--}6\%$ . The top boundary of this region is poorly defined, with the film quality gradually becoming more nanocrystalline with increasing CH<sub>4</sub> concentration until either the filament becomes covered in soot ending film growth, or graphitic films are deposited. The lower boundary appears to be much sharper, with the film quality changing from MCD to ‘no growth’ within less than 1% change in CH<sub>4</sub> concentration. Very close to the boundary between MCD and ‘no growth’, we observe some NCD film deposition. The evidence for NCD was taken as the presence of the 1150–1190 cm<sup>−1</sup> Raman line (see Figs. 4 and 5). The growth rate of NCD films in this boundary region was low, around 0.1 μm h<sup>−1</sup>. Immediately below the boundary, i.e. just inside the ‘no growth’ region, we often observed isolated nanoparticles lying on the surface, but which appeared not to be bonded to the surface (see Fig. 1(b)).

## 5. Discussion

Some questions arise from these findings. Why is it that gas compositions such as 1%CH<sub>4</sub>/Ar (with or without 1–2% added H<sub>2</sub>) grow UNCD films in a MW reactor, but the same gas composition in a hot filament reactor produces only graphitic films? In other words, why does the idea behind the Bachmann diagram, which works for the H-rich

gas mixtures, fail for these Ar-rich/H-poor gas mixtures? Is there some difference between the gas phase chemistry in the two reactors in the Ar/CH<sub>4</sub>/H<sub>2</sub> system?

The results from the computer modelling of the gas phase composition may help to answer these questions. There are three major differences between MW plasma activation and hot filament activation of these types of gas mixtures at these pressures. The first is that the MW system has much more input power than a HF system, 800 W compared to ~120 W, respectively. Thus gas mixture activation is liable to be far more extensive in a MW system, as well as it having a higher overall gas temperature.

Second, a HF system relies only upon thermal energy and catalytic H<sub>2</sub> dissociation on the filament surface to initiate the gas phase chemistry, whereas for a MW system, in addition to thermal activation, there are plasma activation processes e.g. direct electron impact excitation and ionisation, and reactions between molecules, ions and excited atoms. For example, previous calculations [22] for MW and DC discharges used to grow CVD diamond showed that electron impact on H<sub>2</sub> was the dominating mechanism for dissociation at low temperature. Thermal dissociation became comparable with electron impact dissociation only at much higher temperatures,  $T_{\text{gas}} > 2800\text{--}3000$  K. Thus MW plasmas will be considerably more efficient at producing radicals and ions than hot filament reactors, especially at lower gas temperatures.

The third major difference between the two reactor systems is in the gas temperature distribution. The hot filament system has a localised source of heat (the filament), and the gas temperature drops off rapidly with distance away from this. The rate of drop-off depends upon the thermal conductivities of the components of the gas mixture, as well as the position and temperature of the substrate. Fig. 2 shows the calculated temperature distribution for a 1%CH<sub>4</sub>/Ar gas mixture, with the filament

temperature at 2400 K and a substrate at a distance of 5 mm maintained at a temperature of 1130 K. The figure also shows the corresponding curve for the same gas mixture in a 800 W MW system. The plot shows that, for conditions closely resembling those in our HF reactor, the gas temperature drops off rapidly at distances away from the filament, reaching <1200 K for gas 1 mm above the growing surface. It is known from previous experimental [2,20] and theoretical [9,23] studies of 1%CH<sub>4</sub>/H<sub>2</sub> mixtures that a gas temperature of >1400 K is needed for efficient thermal dissociation of H<sub>2</sub> which can then subsequently react with gas phase hydrocarbons to release the diamond growth precursor, CH<sub>3</sub>. The calculations show that temperatures in excess of this only occur within 2.5 mm of the filament. Thus, it is clear that a HF system is very inefficient at producing H atoms near to the substrate surface. Therefore, for growth to occur, the H atoms that are created within the 2.5 mm ‘hot region’ close to the filament need to diffuse through the colder background gas to the surface. Some of them inevitably will be lost via reactions with background gas molecules during this journey. Conversely, the MW plasma is seen to be much

hotter (3000 K) in the centre of the plasma ball, and even with the temperature drop-off toward the substrate, we still calculate a gas temperature of 2000 K within 1 mm of the substrate surface. Thus, the MW system produces gas temperatures at or close to the substrate surface which are significantly hotter than those in a HF system, and thus the important reactions that generate H atoms can occur much closer to the growing surface.

But if there is such a large apparent difference in gas activation in the two reactor types, why then is the growth of MCD films from a standard 1%CH<sub>4</sub>/H<sub>2</sub> gas mixture seemingly independent of reactor type, as the Bachman diagram shows? If the background gas is mostly hydrogen (as in a 1%CH<sub>4</sub>/H<sub>2</sub> gas mixture) then (a) the initial concentration of H atoms created near the filament will be large, and (b) the small collision cross-section for H and H<sub>2</sub> means that the diffusion coefficients of the H atoms will be large. Thus, a high concentration of H atoms will survive the journey from the filament to the substrate surface. Therefore, the rapid temperature drop-off will not significantly affect the H atom concentration near the substrate, and so diamond growth can still occur readily.

Table 1

Species concentration of the gas phase components present in a HF and a MW reactor at 60 Torr, calculated for different input gas mixtures at a position 1 mm above the substrate surface

Species	Hot filament reactor			MW reactor	
	1%CH <sub>4</sub> /H <sub>2</sub>	1%CH <sub>4</sub> /Ar	1%CH <sub>4</sub> /2%H <sub>2</sub> /97%Ar	1%CH <sub>4</sub> /H <sub>2</sub>	1%CH <sub>4</sub> /2%H <sub>2</sub> /97%Ar
	$T_{\text{fil}}=2700 \text{ K}$	$T_{\text{fil}}=2700 \text{ K}$	$T_{\text{fil}}=2700 \text{ K}$	$T_{\text{gas-sub}}=1540 \text{ K},$ 800 W	$T_{\text{gas-sub}}=1816 \text{ K},$ 800 W
	$T_{\text{gas-sub}}=1160 \text{ K}$	$T_{\text{gas-sub}}=1130 \text{ K}$	$T_{\text{gas-sub}}=1163 \text{ K}$	Concentration/cm <sup>-3</sup>	Concentration/cm <sup>-3</sup>
H	$4.00 \times 10^{14}$	$2.78 \times 10^{12}$	$3.98 \times 10^{13}$	$1.73 \times 10^{15}$	$2.68 \times 10^{14}$
CH <sub>3</sub>	$7.64 \times 10^{13}$	$1.01 \times 10^{14}$	$1.76 \times 10^{14}$	$1.33 \times 10^{13}$	$1.20 \times 10^{12}$
C <sub>2</sub> H <sub>2</sub>	$2.56 \times 10^{14}$	$1.89 \times 10^{14}$	$1.97 \times 10^{15}$	$3.19 \times 10^{15}$	$1.98 \times 10^{15}$
CH <sub>2</sub>	$2.37 \times 10^{10}$	$1.16 \times 10^9$	$6.11 \times 10^{10}$	$4.65 \times 10^{10}$	$4.53 \times 10^{10}$
CH	$1.48 \times 10^8$	$3.23 \times 10^6$	$2.10 \times 10^9$	$6.47 \times 10^8$	$3.90 \times 10^9$
C	$5.67 \times 10^{10}$	$6.49 \times 10^4$	$4.27 \times 10^9$	$4.99 \times 10^9$	$5.58 \times 10^{10}$
C <sub>2</sub> (a)	—	$5.79 \times 10^{10}$	$3.27 \times 10^{11}$	$9.74 \times 10^7$	$1.76 \times 10^{10}$
C <sub>2</sub> (X)	—	$2.36 \times 10^{10}$	$1.11 \times 10^{11}$	$5.69 \times 10^6$	$2.28 \times 10^9$
C <sub>2</sub> H	$1.88 \times 10^7$	$1.98 \times 10^9$	$8.75 \times 10^9$	$2.00 \times 10^{10}$	$2.22 \times 10^{12}$
C <sub>2</sub> H <sub>6</sub>	$9.52 \times 10^{12}$	$1.39 \times 10^{14}$	$1.18 \times 10^{14}$	$1.41 \times 10^{10}$	$2.67 \times 10^7$
C <sub>2</sub> H <sub>4</sub>	$4.45 \times 10^{13}$	$1.17 \times 10^{14}$	$1.56 \times 10^{14}$	$3.24 \times 10^{13}$	$2.54 \times 10^{11}$
C <sub>2</sub> H <sub>5</sub>	$1.23 \times 10^{11}$	$8.86 \times 10^{11}$	$1.37 \times 10^{12}$	$4.31 \times 10^9$	$9.88 \times 10^6$
C <sub>2</sub> H <sub>3</sub>	$1.73 \times 10^{11}$	$1.76 \times 10^{11}$	$1.39 \times 10^{12}$	$6.66 \times 10^{11}$	$2.15 \times 10^{10}$
H <sub>2</sub>	$4.94 \times 10^{17}$	$6.55 \times 10^{14}$	$7.02 \times 10^{15}$	$5.81 \times 10^{17}$	$1.72 \times 10^{16}$
CH <sub>4</sub>	$2.96 \times 10^{15}$	$4.47 \times 10^{15}$	$1.54 \times 10^{15}$	$2.06 \times 10^{14}$	$3.22 \times 10^{12}$
Ar	0	$5.05 \times 10^{17}$	$4.87 \times 10^{17}$	0	$5.09 \times 10^{17}$
Ratios					
[H]:[CH <sub>3</sub> ]	5.2	0.028	0.23	130	223
[H]:[C <sub>2</sub> ]	—	34	91	$1.7 \times 10^7$	$1.3 \times 10^4$
[CH <sub>3</sub> ]:[C <sub>2</sub> ]	—	1240	402	$1.3 \times 10^5$	60
Film type	MCD	No growth	No growth	MCD	UNCD

This is a subset of the full calculated species distributions as a function of distance from the substrate, which will appear in a later paper [17].  $T_{\text{gas-sub}}$  is the calculated gas temperature just above the substrate surface, which is much lower than in the centre of the plasma ball or close to the filament. It is worth pointing out that although the calculated C<sub>2</sub> concentration at 1 mm from the substrate in the 1%CH<sub>4</sub>/2%H<sub>2</sub>/97%Ar plasma is only  $\sim 10^{10} \text{ cm}^{-3}$ , in the centre of the plasma ball it is  $\sim 10^{12} \text{ cm}^{-3}$ , which is consistent with the measurements made using laser spectroscopic techniques [10]. Also given in the table are the ratios of the concentrations of atomic H, CH<sub>3</sub> and C<sub>2</sub> for the different conditions. Note that for the two gas compositions containing Ar, which do not give diamond growth in the HF reactor, the [H]:[CH<sub>3</sub>] ratio is less than one. Also, for both reactors and all gas mixtures [CH<sub>3</sub>]:[C<sub>2</sub>] is very large, meaning that C<sub>2</sub> is a minority species near the substrate surface.

However, if the gas mixture is mostly Ar (as in a 1%CH<sub>4</sub>/Ar gas mixture), then the converse is true: (a) the initial concentration of H atoms created near the filament will be low (since the only source of H is from CH<sub>4</sub> which comprises only 1% of the input gas), (b) the larger collision cross-section for Ar means that diffusion coefficients of the H atoms, CH<sub>3</sub> and other radicals in Ar will be ~1.5–3 times lower than in H<sub>2</sub>, and (c) the thermal conduction coefficient in Ar is ~10 times lower than in H<sub>2</sub> and thus the hot region in H<sub>2</sub> will be larger than in Ar. All these factors mean that the H atom concentration at the growth surface is no longer sufficiently high to perform efficiently all the reactions necessary for diamond growth.

Further evidence for this can be obtained by comparing the concentrations of H and CH<sub>3</sub> for a hydrogen-rich system and for an Ar-rich system. Using the computer model outlined above, species concentrations were calculated for a HF system for the two different gas mixtures, and are shown in Table 1. This shows that for the 1%CH<sub>4</sub>/Ar system, the CH<sub>3</sub> concentration at the substrate surface is almost the same (factor of 1.3) as in the 1%CH<sub>4</sub>/H<sub>2</sub> system, but more importantly, that the H atom concentration is a factor of 144 times smaller. In terms of the [H]:[CH<sub>3</sub>] ratio (which plays an important role in determining the growth rate and quality of diamond deposited), this has decreased from 5:1 to 1:36. Since H atoms are believed to be essential in the standard diamond growth mechanism, the scarcity of H atoms explains the poor growth rate, whilst the relative abundance of carbon species explains the tendency to form poor quality diamond, nanodiamond or graphite. Adding extra H<sub>2</sub> to the gas mixture improves matters, since this affects the initial concentration of H atoms, and so we see some diamond deposition, although the growth rates remain slow, and the diamond quality is poor or nanocrystalline.

The situation is different for MW plasma systems because of the spatially distributed source of the radicals and the different temperature distribution. In most MW systems, the plasma ball extends to ~1 mm from the substrate surface, and in some cases the substrate is even immersed in the edges of the plasma. Thus, the hot region is much closer to the substrate in MW systems than in HF systems (see Fig. 2). Measurements of plasma temperatures in 1%CH<sub>4</sub>/Ar plasmas have yielded values between 1600 K [21] and 3000 K [10], which is sufficient to thermally dissociate H<sub>2</sub>. Since this occurs very close to the diamond surface, the resulting H atoms can diffuse there readily and perform the H-abstraction reactions necessary for diamond growth. This process can also be improved by addition of extra H<sub>2</sub>, hence the observation of increased ‘quality’ of diamond and the transition from NCD to MCD with added H<sub>2</sub> [24].

Also from Table 1 we can determine the relative importance of other gas phase species. For example, in a MW reactor using the standard UNCD growth mixture of 1%CH<sub>4</sub>/2%H<sub>2</sub>/97%Ar, the concentration of C<sub>2</sub> is a factor of 100 times smaller than that of either CH<sub>3</sub> or C<sub>2</sub>H, which

suggests that C<sub>2</sub> may be much less important for the growth of UNCD than the other two radicals.

## 6. Conclusions

We have extended the compositional map of Lin et al. [11] for the Ar/CH<sub>4</sub>/H<sub>2</sub> system in a HF reactor to the gas mixing ratios commonly used to grow NCD and UNCD in MW reactors. We find that NCD growth is confined to a limited composition window at the boundary between the MCD growth region and the ‘no growth’ region, and the NCD growth rates are very small (<0.1 μm h<sup>-1</sup>). The reason for this has been rationalised in terms of the degree of gas mixture activation combined with the gas temperature distribution within a HF reactor causing a substantial reduction in the concentration of H atoms along with a decrease in the [H]:[CH<sub>3</sub>] ratio near to the growing substrate surface. The implications for successful (high growth rate) UNCD deposition in HF reactors are therefore not promising. In order to create the necessary concentrations of the growth species at the substrate surface, we would require a filament temperature of >3000 K, which is prohibitively high, even for high-boiling-point metals such as tungsten. Alternatively, placing the filament closer to the substrate would help, but this would be at the expense of growth area which would then be limited to only a few square millimetres.

## Acknowledgments

The authors would like to thank Professor Mike Ashfold, Edward Crichton and other members of the Bristol diamond group for useful discussions. James Smith wishes to thank the EPSRC for funding under the Carbon Based Electronics initiative. Yuri Mankelevich wishes to thank RFBR for Key Science Schools Grant No. 1713.2003.2 and I.A.S. for the Benjamin Meaker visiting professorship award.

## References

- [1] P.W. May, Philos. Trans. R. Soc. Lond., A 358 (2000) 473.
- [2] C.A. Rego, P.W. May, C.R. Henderson, M.N.R. Ashfold, K.N. Rosser, N.M. Everitt, Diamond Relat. Mater. 4 (1995) 770.
- [3] S.M. Leeds, P.W. May, E. Bartlett, M.N.R. Ashfold, K.N. Rosser, Diamond Relat. Mater. 8 (1999) 1377.
- [4] P.K. Bachmann, D. Leers, H. Lydtin, Diamond Relat. Mater. 1 (1991) 1.
- [5] S.J. Harris, Appl. Phys. Lett. 56 (1990) 2298.
- [6] D.G. Goodwin, J.E. Butler, in: M.A. Prelas, G. Popovici, L.K. Bigelow (Eds.), *Handbook of Industrial Diamonds and Diamond Films*, Marcel Dekker, New York, 1998.
- [7] X. Xiao, J. Birrell, J.E. Gerbi, O. Auciello, J.A. Carlisle, J. Appl. Phys. 96 (2004) 2232.
- [8] D. Zhou, T.G. McCauley, L.C. Qin, A.R. Krauss, D.M. Gruen, J. Appl. Phys. 83 (1998) 540.

- [9] E. Crichton, P.W. May, unpublished results presented at ICNDST-9, Tokyo, April 2004, and Diamond 2004, Italy.
- [10] J.R. Rabeau, P. John, J.I.B. Wilson, Y. Fan, *J. Appl. Phys.* 96 (2004) 6724.
- [11] T. Lin, G.Y. Yu, A.T.S. Wee, Z.X. Shen, *Appl. Phys. Lett.* 77 (2000) 2692.
- [12] Y.A. Mankelevich, A.T. Rakhimov, N.V. Suetin, *Diamond Relat. Mater.* 7 (1998) 1133.
- [13] G.P. Smith, D.M. Golden, M. Frenklach, N.W. Moriarty, B. Eiteneer, M. Goldenberg, C.T. Bowman, R.K. Hanson, S. Song, W.C. Gardiner, Jr., V.V. Lissianski, Z. Qin, <http://www.me.berkeley.edu/gri-mech/>.
- [14] Y.A. Mankelevich, N.V. Suetin, M.N.R. Ashfold, J.A. Smith, E. Cameron, *Diamond Relat. Mater.* 10 (2001) 364.
- [15] M.N.R. Ashfold, P.W. May, J.R. Petherbridge, K.N. Rosser, J.A. Smith, Y.A. Mankelevich, N.V. Suetin, *Phys. Chem. Chem. Phys.* 3 (2001) 3471.
- [16] J.A. Smith, J.B. Wills, H.S. Moores, A.J. Orr-Ewing, Yu. A. Mankelevich, N.V. Suetin, *J. Appl. Phys.* 92 (2002) 672.
- [17] Yu. A. Mankelevich, et al., in preparation.
- [18] A.G. Engelhardt, A.V. Phelps, *Phys. Rev.* 131 (1963) 2115; A.V. Phelps, J.I.L.A. Information Center Report, N28, (1985).
- [19] C.J. Rennick, R. Engeln, J.A. Smith, A.J. Orr-Ewing, M.N.R. Ashfold, *J. Appl. Phys.* 97 (2005) 113306.
- [20] M.N.R. Ashfold, A.J. Orr-Ewing, Yu. A. Mankelevich et al., (in preparation).
- [21] A.N. Goyette, J.E. Lawler, L.W. Anderson, D.M. Gruen, T.G. McCauley, D. Zhou, A.R. Krauss, *J. Phys. D: Appl. Phys.* 31 (1998) 1975.
- [22] S.V. Kostiuk, Yu. A. Mankelevich, N.V. Suetin, A.T. Rakhimov, 1998, Proc. Electrochem. Soc., PV 97-32, (Diamond Materials V; Paris; France; 1997), p. 152.
- [23] R.S. Tsang, PhD Thesis, Characterisation of the gas-phase environment in a hot filament diamond chemical vapour deposition chamber using molecular beam mass spectrometry, University of Bristol, School of Chemistry, UK, August 1997 [<http://www.chm.bris.ac.uk/pt/diamond/polysynthesis/intro.htm>].
- [24] J. Birrell, J.E. Gerbi, O. Auciello, J.M. Gibson, J. Johnson, J.A. Carlisle, *Diamond Relat. Mater.* 14 (2005) 86.